SEMARAK ILMU PUBLISHING

Journal of Advanced Research in Applied Mechanics

Journal homepage:
https://semarakilmu.com.my/journals/index.php/appl_mech/index
ISSN: 2289-7895


# Determination of the Anand Parameters for SAC405 Solders through the Use of Stress-Strain Data

Mohd Syafiq Azfar Rizaman[1], Ahmad Sufian Abdullah[1,2,*], Aliff Farhan Mohd Yamin[1,2]

[1] Centre for Mechanical Engineering Studies, Universiti Teknologi MARA, Cawangan Pulau Pinang, 13500, Malaysia
[2] Advanced Mechanics Research Group, Centre for Mechanical Engineering Studies, Universiti Teknologi MARA, Cawangan Pulau Pinang, 13500, Malaysia

**ARTICLE INFO**

***Article history:***
Received 30 September 2023
Received in revised form 2 December 2023
Accepted 20 December 2023
Available online 19 January 2023

***Keywords:***
Anand model; SAC405; Inelastic Constitutive Model

**ABSTRACT**

The Anand inelastic constitutive model is commonly employed to depict the deformation behaviour of solders in electronics components. In the Anand model, plasticity and creep are coupled and described by the same set of flow and evolution relations. Literature study reveals that researchers have calculated varying values for the Anand model parameters when describing different SAC solders. Using Anand's constitutive model for SAC405 (95.5Sn-4.0Ag-0.5Cu) lead-free solder, the theoretical equations for the solder's uniaxial stress-strain response were obtained in this paper. The steps to obtain the parameters of Anand model using stress-strain were also determined. Data on uniaxial stress and strain at various temperatures (T = 298 K (25 °C), 323 K (50 °C), 348 K (75 °C), 373 K (100 °C), and 398 K (125 °C)) and strain rates ($\dot{\varepsilon}$ = 1 × $10^{-3}$ $sec^{-1}$, 1 × $10^{-4}$ $sec^{-1}$, and 1 × $10^{-4}$ $sec^{-1}$) was used to calculate the Anand parameters. The Anand model's accuracy (goodness of fit) with the retrieved parameters was assessed by comparing the model's findings to the observed stress-strain data. The Anand model consistently generated good predictions of the empirical data in all cases, across a wide range of temperatures and stress-strain levels. The goodness of fit values obtained were 0.992, 0.983 and 0.982 for strain rate 1 × $10^{-3}$ $sec^{-1}$, 1 × $10^{-4}$ $sec^{-1}$ and 1 × $10^{-5}$ $sec^{-1}$ respectively.

## 1. Introduction

Electronic packaging necessitates the long-term reliability of solder joints. In the real world, solder joint failure is typically the result of complex mechanisms involving the interaction of numerous fundamental failure processes [1]. The most prevalent failure modes are insufficient alloy mechanical strength due to fatigue, creep due to excessive intermetallic compound production, voids, and leaching [2]. The phenomenon of weariness, particularly heat exhaustion, has garnered much attention. However, there are minimal data on creep and stress deformation in conventional solder alloys [3]. Diverse constitutive models for creep have been developed to characterize the stress–strain relationship during creep and to represent the material's creep properties [4]. Ma *et al.,* have conducted a comprehensive analysis of the mechanical properties and behaviors of lead-free

* *Corresponding author.*
*E-mail address: ahmadsufian@uitm.edu.my*

https://doi.org/10.37934/aram.113.1.162175

solders. They demonstrated that age-dependent inelastic constitutive equations are crucial for Sn-Ag-Cu (SAC) lead-free solders. There are numerous approaches to constitutive modelling of microelectronic solders described in the literature [5]. Solomon utilized a straightforward power law model to describe the interdependence among shear stress, shear strain and shear strain rate. The individual exhibited that solder containing significant proportion of lead had greater resistance to variations in temperature and strain rate as compared to solder composed of a Tin-Lead alloy. [6]. In order to account for the stress-dependence of the activation energy and the strong Bauschinger effect, Busso *et al.,* published a continuum-theory-based inelastic model for Tin-Lead solder. The model discussed in the study focused on the incorporation of the kinematic hardening rule and static recovery factors [7].

The Anand model's ability to forecast plasticity and creep, as well as its incorporation into a number of commercial finite element software packages, have made it an appealing option among engineers working with Tin-Lead and lead-free solders. Developed by Anand and Brown, the Anand model is one of the most popular constitutive models used to de-scribe the mechanical properties of solder [8]. The Anand model is typically employed to represent solder deformation in electronic packages [9]. High-temperature (above 0.5 $T_m$) rate-dependent deformation of metals is described by a well-known set of inelastic constitutive equations that were introduced by Anand [10]. There are two key features that set the Anand model apart from competing constitutive models. To begin, the yield condition or loading and unloading requirements are not necessary in this constitutive model. Second, the average isotropic deformation resistance to macroscopic plastic flow is expressed as a scalar in the model [11]. When utilizing the Anand model to characterize the inelastic deformation of solders, it is imperative to consider many physical variables, including temperature history effects, temperature sensitivity, strain rate sensitivity, strain hardening, and strain rate [12]. The application of finite elements enables the utilization of the unified Anand model for the purpose of characterizing the inelastic deformation of solder alloys and simulating the stress-strain responses shown by solder joints during their operational lifespan [13]. Plasticity and creep are explained by the same set of flow and evolution relations in the Anand model, making it a unified model.

The Anand model has been used by numerous researchers for applications in electronic packaging. Che *et al.,* established four unique constitutive models for the Sn3.8Ag0.7Cu solder alloy. They showed that the Anand model was in line with predictions for the fatigue life of lead-free solders compared to elastic-plastic, elastic-creep, elastic plastic with creep models [14]. To account for temperature effects on one of the model parameters ($h_0$), Chen *et al.,* developed an updated version of the Anand constitutive model [15]. Amagai *et al.,* determined the Anand model parameters for the lead-free solders Sn-3.5Ag-0.75Cu and SAC105 (Sn-1.0Ag-0.5Cu). Eight from the nine required parameters were detailed, however one was left out of their work which was $s_0$ [16]. Kim, *et al.,* reported values for all nine parameters for Sn-1.0Ag-0.5Cu lead free solder [17]. Bai *et al.,* provided an improved version of the Anand model for the lead-free solders SAC305 (Sn-3.0Ag-0.5Cu) and Sn-3.5Ag-0.7Cu. Their method involved utilizing values that were temperature and strain-rate dependent for model parameter $h_0$ [18]. Jurgen Wilde also incorporated Anand parameters that were determined to predict both the stress strain curve and the creep behavior of 92.5Pb-5Sn-2.5Ag using the same set of parameters [19]. In addition to this, the Anand model has seen widespread use in the simulation of solder joints in electronics components, which is done with the help of finite elements [20, 21].

Literature study shows that the researchers have calculated varying values for the Anand model parameters when describing distinct SAC solders. Moreover, it is apparent that the computed model parameters for the same SAC alloy vary considerably across study groups. The determination of the nine parameters of the Anand model is commonly achieved by conducting uniaxial stress-strain

experiments at various strain rates and temperatures, employing a traditional multistep technique. Despite the prevalence of creep data collection for solders, its use in determining Anand model parameters is somewhat unusual.

In this study, the Anand inelastic constitutive model was used to derive the theoretical equations for the uniaxial stress-strain response. Also, methods were established for extracting the parameters of the Anand model from experimental data. The Anand parameters value for the lead-free solder SAC405 (95.5Sn-4.0Ag-0.5Cu) were calculated after these two methods were established. The Anand parameters was derived from uniaxial stress-strain data that was collected throughout a broad spectrum of strain rates ($\dot{\varepsilon}$ = 1 × $10^{-3}$ $sec^{-1}$, 1 × $10^{-4}$ $sec^{-1}$, and 1 × $10^{-5}$ $sec^{-1}$) and temperatures (T = 298 K, 323 K, 348 K, 373 K and 398 K). The Anand model's accurateness (goodness of fit) employing the retrieved parameters was assessed by comparing the model responses to the recorded stress-strain data.

## 2. Methodology

### *2.1 Data Extraction and Experimental Results*

The data gathering process was conducted in order to acquire as much information as possible regarding the stress strain test. The data collection comprises several sorts of experiments conducted at various temperature ranges. Next, a set of data with varying strain rates was collected to compare the different strain rates that will affect the solder joints' creep mechanism. The acquired data was utilized for curve fitting techniques that extract the parameters of the new constitutive model proposed. Ultimately, the collected data was utilized to validate the dependability of the newly suggested inelastic constitutive model in forecasting the inelastic behavior of solder joints.

Figure 1, 2 and 3 presents three stress-strain curves for SAC405 lead-free solder that was used for the experiment at various temperatures (T = 298 K, 323 K, 348 K, 373 K and 398 K) and strain rates ($\dot{\varepsilon}$ = 1 × $10^{-3}$ $sec^{-1}$, 1 × $10^{-4}$ $sec^{-1}$, and 1 × $10^{-5}$ $sec^{-1}$). The data were gathered from a paper by Munshi Basit and colleagues [22].

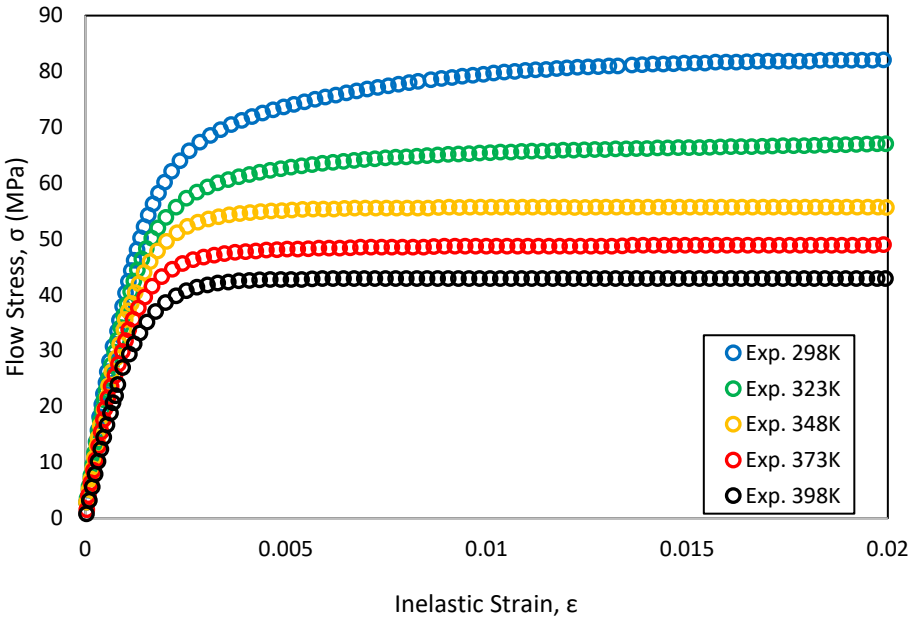


**Fig. 1.** Stress-strain curves of lead-free solder SAC405 at constant strain rate of 1 × $10^{-3}$ $sec^{-1}$ with different temperatures [22]

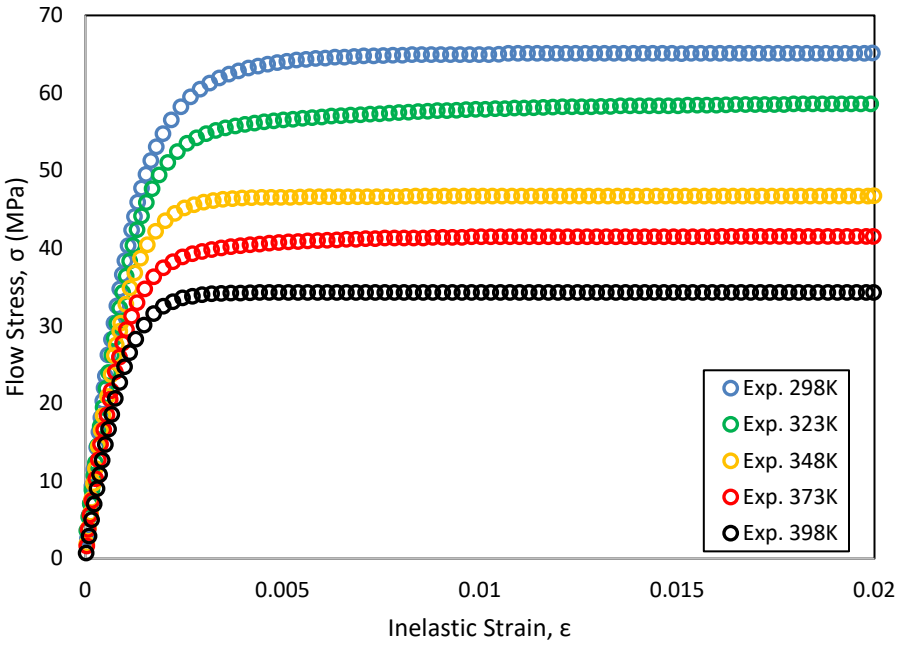


**Fig. 2.** Stress-strain curves of lead-free solder SAC405 at constant strain rate of $1 \times 10^{-4}$ $sec^{-1}$ with different temperatures [22]

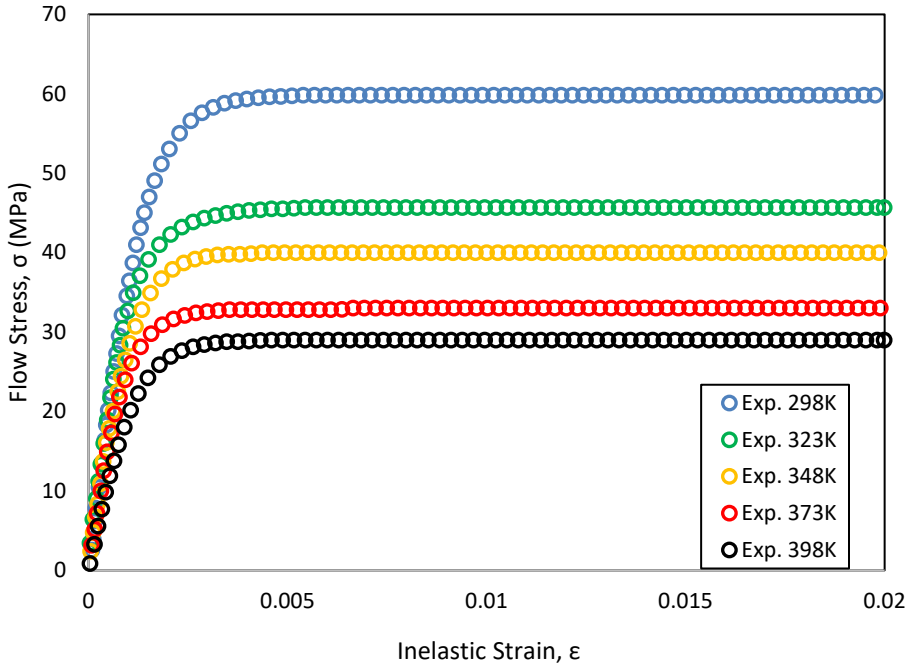


**Fig. 3.** Stress-strain curves of lead-free solder SAC405 at constant strain rate of $1 \times 10^{-5}$ $sec^{-1}$ with different temperatures [22]

### *2.2 0.2% Offset for Yield Stress*

Materials deform and change shape when loaded. Deformations are classified into two which are elastic and plastic. Elastic deformation refers to a reversible alteration in the shape of a material that transpires upon the application of tension, although the material reverts to its initial configuration once the stress is alleviated. The observed behavior adheres to Hooke's law, which asserts that the magnitude of deformation experienced by a material is directly proportional to the magnitude of

stress applied, as long as the material remains within its elastic limit. In contrast, plastic deformation is a type of deformation that is not reversible and takes place when the force applied to the material surpasses its yield strength. When a substance experiences plastic deformation, it develops a persistent alteration in its form, failing to revert to its initial state upon an absence of external stress.

The utilization of the 0.2% offset approach in the analysis of stress-strain curves is attributed to its ability for accurately determining the yield strength of a given material. The yield strength is a fundamental mechanical parameter that signifies the critical point at which a material experiences plastic deformation, hence changing from its elastic phase. By employing the 0.2% offset approach, a specific point on the stress-strain curve may be found where the material starts to deform plastically. This approach provides enhanced clarity, particularly in situations where the curve lacks a pronounced and well-defined yield point. The 0.2% offset provides a standardized and consistent technique, allowing scientists and engineers to examine materials and assess their appropriateness for various applications.

In order to implement the 0.2% offset method, the stress-strain curve is plotted and the linear elastic region, where stress and strain are proportional, is identified. Then, a line parallel to this region is drawn, shifted by 0.2% strain (0.002 in strain units). At the intersection of this line and the stress-strain curve, the 0.2% offset yield strength is measured. The Figure 4, 5 and 6 below show the new stress strain curves for all three strain rates after the 0.2% offset method has been employed.

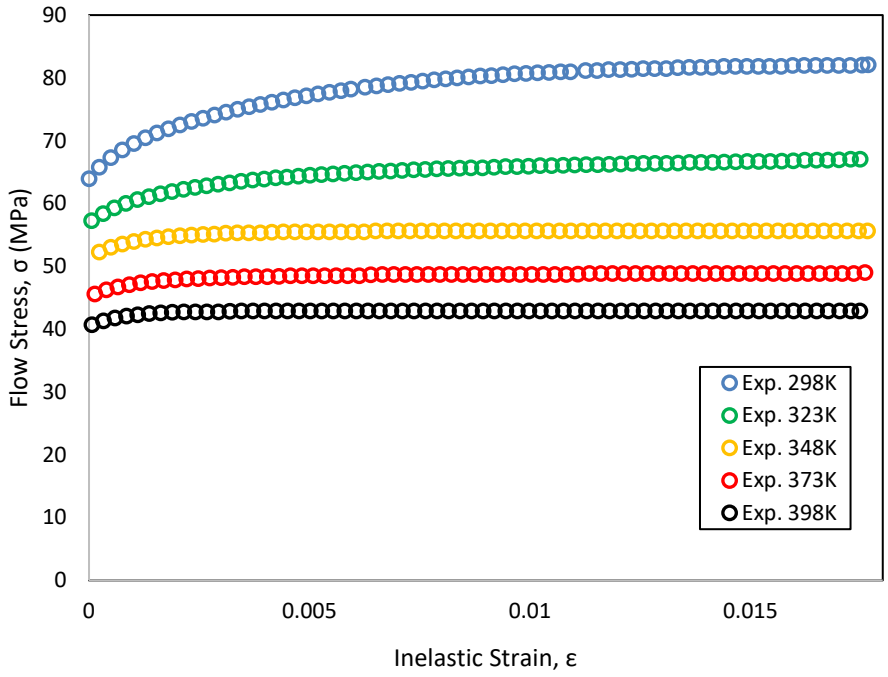


**Fig. 4.** Stress-strain curves of lead-free solder SAC405 at constant strain rate of $1 \times 10^{-3}$ $sec^{-1}$ with different temperatures [22] with 0.2% offset

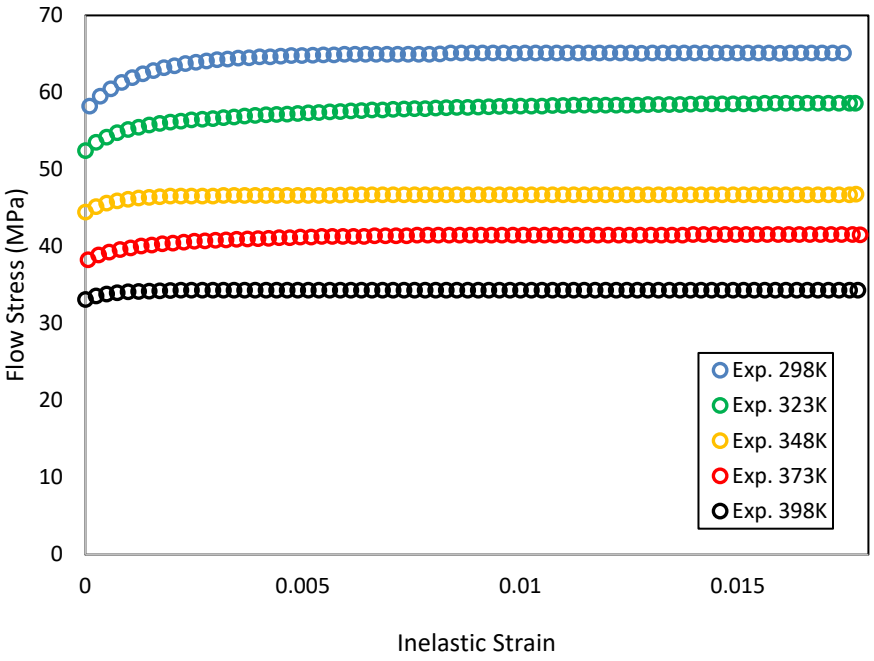


**Fig. 5.** Stress-strain curves of lead-free solder SAC405 at constant strain rate of $1 \times 10^{-4}$ $sec^{-1}$ with different temperatures [22] with 0.2% offset

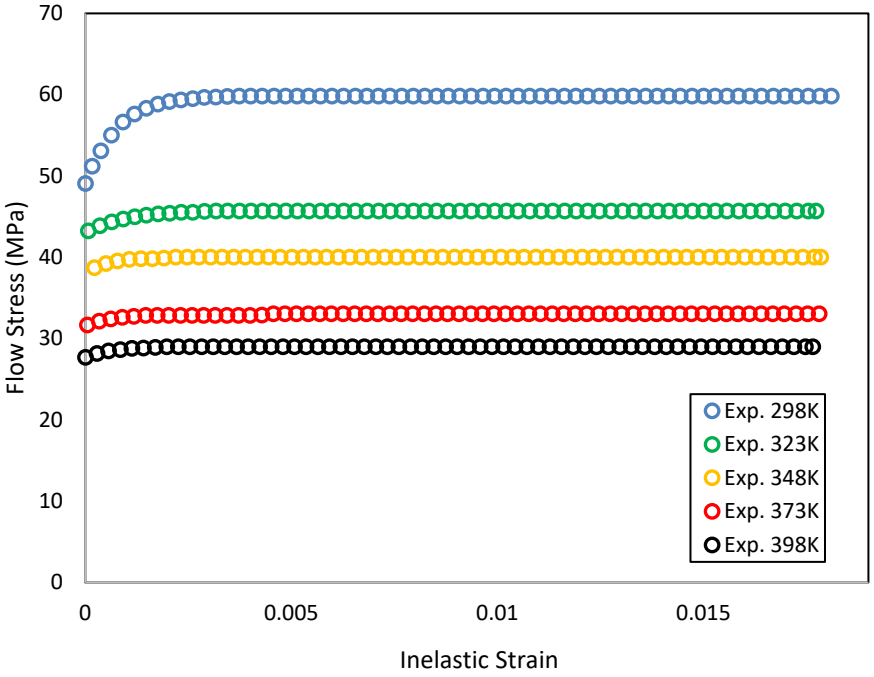


**Fig. 6.** Stress-strain curves of lead-free solder SAC405 at constant strain rate of $1 \times 10^{-5}$ $sec^{-1}$ with different temperatures [22] with 0.2% offset

### *2.3 Anand Inelastic Constitutive Model*

The isotropic resistance of the internal state to plastic flow is represented in the Anand model by the scalar internal variable s. Solder's creep and rate-dependent plastic behavior are brought under a single theoretical roof by using a stress equation and integrating a flow equation and an evolution equation [23]. Neither a loading criterion nor a yield condition are required in this model.

Eq. (1) below shows the equivalent stress equation for the one-dimensional case (uniaxial loading).

$$\sigma = cs; \;\; c < 1 \tag{1}$$

where σ is the equivalent stress for steady plastic flow, s is the internal variable and c is the function of temperature and strain rate which can be stated as Eq. (2).

$$C = \frac{1}{\xi} sinh^{-1}\left\{\left[\frac{\dot{\varepsilon}_{in}}{A} exp\left(\frac{Q}{RT}\right)\right]^{m}\right\} \tag{2}$$

where ξ is the multiplier of stress, $\dot{\varepsilon}_{in}$ is the inelastic strain rate, A is the pre-exponential factor, Q is the activation energy, R is the universal gas constant, T is the absolute temperature and m is the strain rate sensitivity.

When Eq. (2) is substituted into Eq. (1), the equivalent stress equation becomes

$$\sigma = \frac{s}{\xi} \sinh^{-1}\left\{\left[\frac{\dot{\varepsilon}_{in}}{A} exp\left(\frac{Q}{RT}\right)\right]^{m}\right\} \tag{3}$$

By rearranging Eq. (3) and finding the strain rate, the Anand model's flow equation will be obtained. As a result, the Anand model can be expressed as Eq. (4).

$$\dot{\varepsilon}_{in} = Aexp\left(-\frac{Q}{RT}\right)\left[\sinh\left(\xi\frac{\sigma}{s}\right)\right]^{\frac{1}{m}} \tag{4}$$

The following is the expression for the evolution equation for the internal variable, ṡ.

$$\dot{s} = \left\{h_0\left|1 - \frac{s}{s^*}\right|^{a} sign\left(1 - \frac{s}{s^*}\right)\right\}\dot{\varepsilon}_{in} \tag{5}$$

With the saturation value of s, $s^*$ is given by:

$$s^* = \hat{s}\left[\frac{\dot{\varepsilon}_{in}}{A} exp\frac{Q}{RT}\right]^{n} \tag{6}$$

where $h_0$ and a are material parameters, ŝ is a coefficient of saturation and n is the strain rate sensitivity for the saturation value of deformation resistance. Eq. (5) can be integrated to yield the final version of the evolution equation for the internal variable s

$$s = s^* - \left[(s^* - s_0)^{(1-a)} + (a-1)\left\{(h_0)(s^*)^{-a}\varepsilon_p\right\}\right]^{\frac{1}{1-a}} \tag{7}$$

The final equations in the Anand constitutive model are the stress equation in Eq. (3), the flow equation in Eq. (4), and the integrated equation in Eq. (7). These expressions include the nine material parameters: A, ξ, Q/R and m in Eq. (3) and (4); and parameters $h_0$, a, $s_0$, ŝ and n in Eq. (7).

To obtain the formula of the saturation stress, $\sigma^*$, Eq. (1), Eq. (2) and Eq. (4) are derived, together with $\sigma^* = cs^*$, are as follows.

Substitute Eq. (2) into Eq. (1)

$$\sigma^* = \frac{s^*}{\xi} sinh^{-1}\left[\frac{\dot{\varepsilon}_{in}}{A} exp\left(\frac{Q}{RT}\right)\right]^m \tag{8}$$

Substitute Eq. (6) into Eq. (8)

$$\sigma^* = \frac{\hat{s}}{\xi}\left[\frac{\dot{\varepsilon}_p}{A} exp\left(\frac{Q}{RT}\right)\right]^n sinh^{-1}\left[\frac{\dot{\varepsilon}_{in}}{A} exp\left(\frac{Q}{RT}\right)\right]^m \tag{9}$$

The saturation stress, temperature, and strain rate are all included in Eq. (9). We can derive the following equations from Eq. (1) and Eq. (5) under isothermal and $s^* > s$ conditions.

$$\sigma = c\left[h_0\left|1 - \frac{s}{s^*}\right|^a sign\left(1 - \frac{s}{s^*}\right)\right]\dot{\varepsilon}_{in} \tag{10}$$

To perform differentiation of stress, σ with respect to strain rate, $\dot{\varepsilon}_{in}$, the parameters of s need to change to σ, and $s^*$ needs to change to $\sigma^*$.

$$\therefore\ \sigma = c\left[h_0\left|1 - \frac{\sigma}{\sigma^*}\right|^a sign\left(1 - \frac{\sigma}{\sigma^*}\right)\right]\dot{\varepsilon}_{in} \tag{11}$$

$$\frac{d\sigma}{d\dot{\varepsilon}_{in}} = c\left[h_0\left|1 - \frac{\sigma}{\sigma^*}\right|^a sign\left(1 - \frac{\sigma}{\sigma^*}\right)\right] \tag{12}$$

Integrating Eq. (12) yields the following form:

$$\sigma = \sigma^* - \left[(\sigma^* - cs_0)^{(1-a)} + (a-1)\{(ch_0)(\sigma^*)^{-a}\}\varepsilon_{in}\right]^{\frac{1}{(1-a)}} \tag{13}$$

In which $s_0$ is the starting value of s and $\sigma_0 = cs_0$. The material parameters $ch_0$, $cs_0$ ($\sigma_0$), and a will be calculated using Eq. (13). In these constitutive equations, the following material parameters must be determined: A, Q, m, n, ξ, ŝ, a, $h_0$ and $s_0$. The starting value of the deformation resistance is given by $s_0$.

### *2.4 Procedures for Determining the Model Parameters Based on the Data from the Stress-Strain Curve*

The practical applicability of a model relies heavily on how straightforward it is to establish the values for the model's material parameters. The Anand inelastic constitutive model includes nine parameters, but their determination is straightforward as all that is needed is data from experiments at different temperatures and strain rates. A, Q/R, ŝ/ξ, $h_0$, ξ, m, n, a and $s_0$ are all material properties that can be resolved using the methods outlined below:

i. Obtain the stress and strain result from the experiment for each temperature and strain rates.

ii. Calculate the constant value of parameter $s^*$ for each temperature and strain rate by using the Eq. (6) given above using the Anand model parameters that have been predicted based on Table 1.
iii. Next, using the obtained value of parameter $s^*$ from (2), the internal variable s is calculated by using the Eq. (7).
iv. The parameter c is determined by using Eq. (2) as mentioned above. After proving that parameter c has a value of less than unity, the predicted stress is then calculated using Eq. (1).
v. A non-linear least square fit method is then used to find all the nine Anand model parameters simultaneously.

In order to make an accurate prediction, the values of the Anand parameters should fall within a particular range, as indicated by previous research. Table 1 provides the allowed values for each Anand model parameter in SAC405 lead-free solder.

**Table 1**
Minimum and maximum values for each anand model parameters

| Symbols | Anand Parameters | Minimum | Maximum |
|---|---|---|---|
| $s_0$ | Internal variable | 10 | 100 |
| Q/R | Activation energy and universal gas constant | 5000 | 15000 |
| A | Pre-exponential factor | 1000 | 10000 |
| ξ | Multiplier of stress | 1 | 10 |
| m | Strain rate sensitivity | 0.05 | 0.5 |
| $h_0$ | Material parameters | 50000 | 250000 |
| $\hat{s}$ | Coefficient of saturation | 10 | 100 |
| n | Strain rate sensitivity for the saturation value of deformation resistance | 0.0001 | 0.1 |
| a | Material parameters | 1 | 5 |

## 3. Results and Discussion

The material parameters for SAC405 lead-free solder material were calculated using the aforementioned method and are presented in Table 2 below.

**Table 2**
Anand model parameters determined for SAC405 from stress-strain data

| Symbols | Anand Parameters | Units | Values |
|---|---|---|---|
| $s_0$ | Internal variable | MPa | 76.675 |
| Q/R | Activation energy and universal gas constant | 1/K | 10573 |
| A | Pre-exponential factor | $sec^{-1}$ | 1557.67 |
| ξ | Multiplier of stress | Dimensionless | 8.52 |
| m | Strain rate sensitivity | Dimensionless | 0.3097 |
| $h_0$ | Material parameters | MPa | 229749 |
| $\hat{s}$ | Coefficient of saturation | MPa | 67.84 |
| n | Strain rate sensitivity for the saturation value of deformation resistance | Dimensionless | 0.0159 |
| a | Material parameters | Dimensionless | 2.031 |

Once the parameters are collected, the stress-strain curve may be predicted using the constitutive model at each temperature and strain rate recorded in the experiment. Correlating the Anand model's stress-strain curves with the experimental stress-strain curves allows the constitutive model's fit to the experimental data to be analyzed. Figures 7, 8, and 9 illustrate the correlation between the experimental results obtained for the five tested temperatures and three strain rates, and the stress-strain curves predicted by the Anand model. There is consistent evidence of a high degree of correlation between the derived Anand model parameters and the experimentally determined test data in each case.

Based on the figures shown, it can be seen that the Anand prediction results in a high goodness of fit value of above 0.9 for all three constant strain rates. Figure 7 of strain rate $1 \times 10^{-3}$ $sec^{-1}$ have an average goodness of fit value of 0.992, while 0.983 for strain rate $1 \times 10^{-4}$ $sec^{-1}$ shown in Figure 8. The average goodness of fit value for the strain rate $1 \times 10^{-5}$ $sec^{-1}$ shown in Figure 9 is 0.982. Consequently, it can be argued that the Anand model possesses the capability to accurately forecast the stress-strain behavior of materials. Next, the data show that the Anand model is more accurate at higher temperatures than at lower temperatures in predicting the stress-strain response. This is evidence from all three stress-stain rates of Figure 7, 8 and 9. Figure 7 also showed the best accuracy compared to both Figure 8 and 9. As seen from the figure, almost all the temperatures for strain rate $1 \times 10^{-3}$ $sec^{-1}$ can be predicted accurately.

Although the figures above demonstrate how the Anand model can simulate non-linear deformation behavior at various temperatures and strain rates while maintaining a very good accuracy with a high goodness of fit value. However, it is not considered that the Anand model fitting outcome to be ideal. One can see that there are certain differences between the experimental data and the data from the real world, and vice versa. The results show that, especially at high homologous temperatures, the Anand model is not very good at characterizing the cross-dependent relationship between temperature and strain rate.

$h_0$ and a are two important parameters that affect the shape of the stress-strain curve. It is possible to make more accurate predictions of the experimental results if a is assumed to be constant and consider $h_0$ to be a function of temperature and strain rate.

When $h_0$ is a constant and a is a variable, it is not always possible to obtain a close approximation of the stress-strain curve. The constant plastic flow state is typically reached at strains around two percent for lead-free solders, allowing the value of the saturation stress to be established at an earlier stage. Although strain hardening behavior was observed at low temperatures, lead-free solder's remarkable stability suggests that the material may attain a steady state in under 60 seconds. The parameter a did not vary much with temperature and strain rate, while $ch_0$ varied greatly with each test throughout the whole process of nonlinear fitting to Eq. (13) of the stress-strain curve shown in Figures 7, 8, and 9. The Anand model can be adjusted by correlating $h_0$ with temperature and strain rate in future studies.

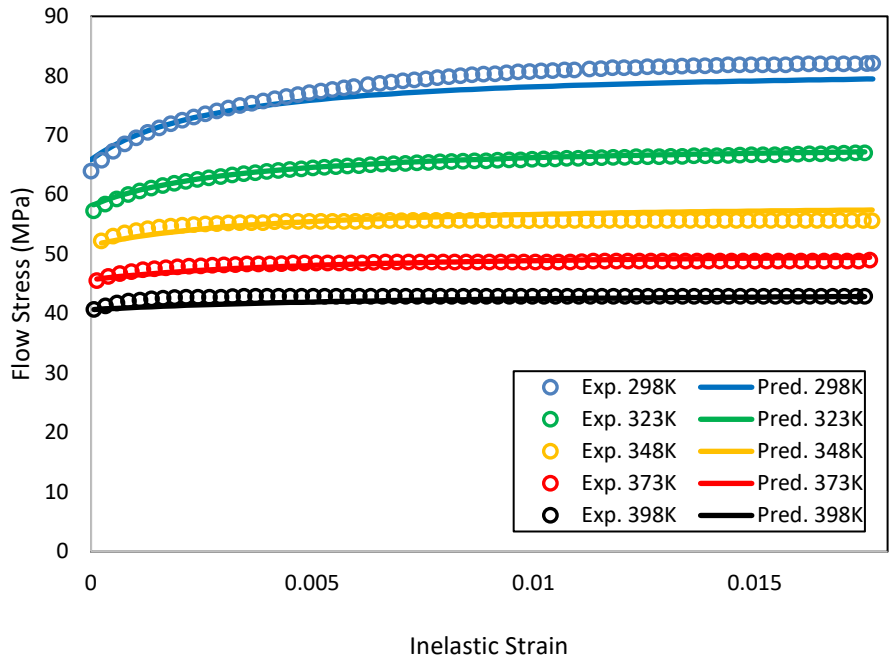


**Fig. 7.** The comparison of experiments [22] and predictions of anand model for lead free solder SAC405 for constant strain rate of $1 \times 10^{-3}$ $sec^{-1}$ with different temperatures

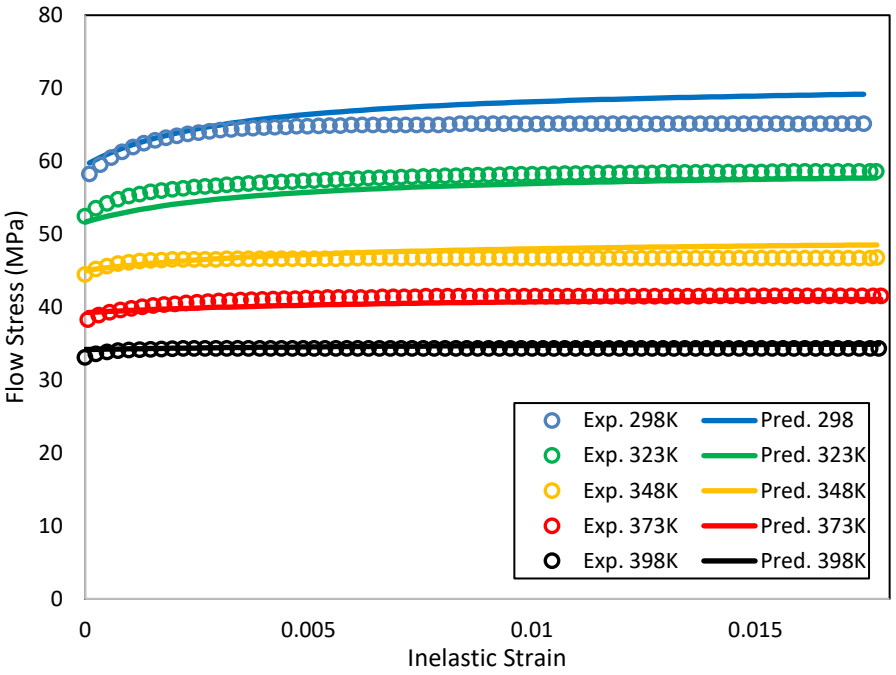


**Fig. 8.** The comparison of experiments [22] and predictions of anand model for lead free solder SAC405 for constant strain rate of $1 \times 10^{-4}$ $sec^{-1}$ with different temperatures

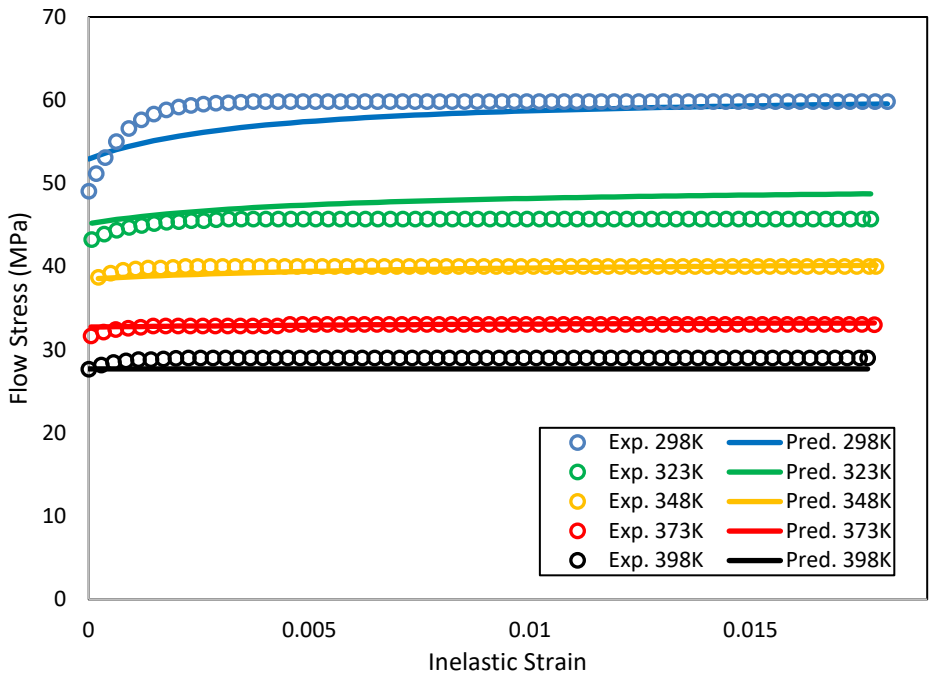


**Fig. 9.** The comparison of experiments [22] and predictions of anand model for lead free solder SAC405 for constant strain rate of $1 \times 10^{-5}$ $sec^{-1}$ with different temperatures

## 4. Conclusions

The Anand inelastic constitutive model was used to calculate the uniaxial stress-strain curve in this study. In addition to this, the processes by which the Anand model parameters can be obtained from experimental data on stress-strain curve have been worked out. The Anand parameters for lead-free solder SAC405 are then calculated using a set of experimental test data using the developed approaches. The Anand parameters were calculated using a variety of strain rates ($\dot{\varepsilon} = 1 \times 10^{-3}$ $sec^{-1}$, $1 \times 10^{-4}$ $sec^{-1}$, and $1 \times 10^{-5}$ $sec^{-1}$) and temperature-dependent (T = 298 K, 323 K, 348 K, 373 K and 398 K) uniaxial stress-strain data.

The numerical magnitudes are very close when the Anand model parameters based on the stress-strain data are compared to the experiment data. In addition, the computed Anand model responses have been assessed to the observed stress-strain data to establish the Anand model's accurateness (goodness of fit) utilizing the retrieved material characteristics. In every instance, the Anand model was proven to accurately replicate the experimental data throughout a broad temperature and stress-strain range of 0.992 for strain rate $1 \times 10^{-3}$ $sec^{-1}$, 0.983 for strain rate $1 \times 10^{-4}$ $sec^{-1}$ and 0.982 for strain rate $1 \times 10^{-5}$ $sec^{-1}$.

## Acknowledgement

This project is funded by the Ministry of Higher Education (MOHE) of Malaysia, ref no. FRGS/1/2021/TK0/UiTM/03/11. Thank you to Universiti Teknologi MARA, Malaysia for various and generous assistance throughout the project until completion.

## References

[1] Ching, Law Ruen, and Mohd Zulkifly Abdullah. "A Review of Moldflow and Finite Element Analysis Simulation of Chip Scale Packaging (CSP) for Light Emitting Diode (LED)." *Journal of Advanced Research in Fluid Mechanics and Thermal Sciences* 99, no. 1 (2022): 158-173. https://doi.org/10.37934/arfmts.99.1.158173

[2] Anuar, Rabiatul Adawiyah Mohamed, Mohamad Shahrom Hamidin, Saliza Azlina Osman, and Mohamad Hilmi Othman. "Intermetallic Compound Layer Growth at the Interface between Sn-Ag and ENImAg Surface Finish." *International Journal* 8, no. 1.2 (2020). https://doi.org/10.30534/ijeter/2020/0881.220
[3] Hwang, J. S., and R. M. Vargas. "Solder joint reliability—Can solder creep?." *Soldering & Surface Mount Technology* 2, no. 2 (1990): 38-45. https://doi.org/10.1108/eb037718
[4] Liu, D. "Research on damage mechanism and creep properties on the sandston e under combination of axial compression and water pressure." *Sichuan University* (2017).
[5] Ma, Hongtao, and Jeffrey C. Suhling. "A review of mechanical properties of lead-free solders for electronic packaging." *Journal of materials science* 44 (2009): 1141-1158. https://doi.org/10.1007/s10853-008-3125-9
[6] Solomon, H. D. "Creep, strain rate sensitivity and low cycle fatigue of 60/40 solder." (1986): 68-75. https://doi.org/10.1109/TCHMT.1986.1136672
[7] Busso, E. P., M. Kitano, and T. Kumazawa. "A visco-plastic constitutive model for 60/40 tin-lead solder used in IC package joints." (1992): 331-337. https://doi.org/10.1115/1.2904181
[8] Yamin, A. F. M., A. S. Abdullah, M. F. A. Manap, and H. Yusoff. "Failure prediction of the solder joints in the ball-grid-array package under thermal loading." In *Journal of Physics: Conference Series*, vol. 1349, no. 1, p. 012013. IOP Publishing, 2019. https://doi.org/10.1088/1742-6596/1349/1/012013
[9] Yamin, A. F. M., N. N. Azmi, N. A. Norrdin, H. Yusoff, and Cawangan Pulau Pinang. "Modified Anand model parameters for 95.5 Sn-4.0 Ag-0.5 Cu lead-free solder material." In *6th Mechanical Engineering Research Day (MERD) Conference Location Melaka, MALAYSIA*, pp. 142-144. CENTRE ADVANCED RESEARCH ENERGY-CARE Location DURIAN TUNGGAL, 2019.
[10] Motalab, Mohammad, Zijie Cai, Jeffrey C. Suhling, Jiawei Zhang, John L. Evans, Michael J. Bozack, and Pradeep Lall. "Improved predictions of lead free solder joint reliability that include aging effects." In *2012 IEEE 62nd Electronic Components and Technology Conference*, pp. 513-531. IEEE, 2012. https://doi.org/10.1109/ECTC.2012.6248879
[11] Zhang, Liang, Ji-guang Han, Yonghuan Guo, and Cheng-wen He. "Anand model and FEM analysis of SnAgCuZn lead-free solder joints in wafer level chip scale packaging devices." *Microelectronics Reliability* 54, no. 1 (2014): 281-286. https://doi.org/10.1016/j.microrel.2013.07.100
[12] Gao, Hong, and Xu Chen. "Effect of axial ratcheting deformation on torsional low cycle fatigue life of lead-free solder Sn–3.5 Ag." *International Journal of Fatigue* 31, no. 2 (2009): 276-283. https://doi.org/10.1016/j.ijfatigue.2008.08.009
[13] Chen, Xu, Gang Chen, and Masao Sakane. "Prediction of stress-strain relationship with an improved Anand constitutive Model For lead-free solder Sn-3.5 Ag." *IEEE Transactions on Components and Packaging Technologies* 28, no. 1 (2005): 111-116. https://doi.org/10.1109/TCAPT.2004.843157
[14] Che, F. X., H. L. J. Pang, W. H. Zhu, Wei Sun, and Anthony YS Sun. "Modeling constitutive model effect on reliability of lead-free solder joints." In *2006 7th International Conference on Electronic Packaging Technology*, pp. 1-6. IEEE, 2006. https://doi.org/10.1109/ICEPT.2006.359842
[15] Chen, Xu, Gang Chen, and Masao Sakane. "Modified Anand constitutive model for lead-free solder Sn-3.5 Ag." In *The Ninth Intersociety Conference on Thermal and Thermomechanical Phenomena In Electronic Systems (IEEE Cat. No. 04CH37543)*, vol. 2, pp. 447-452. IEEE, 2004.
[16] Amagai, Masazumi, Masako Watanabe, Masaki Omiya, Kikuo Kishimoto, and Toshikazu Shibuya. "Mechanical characterization of Sn–Ag-based lead-free solders." *Microelectronics Reliability* 42, no. 6 (2002): 951-966. https://doi.org/10.1016/S0026-2714(02)00017-3
[17] Kim, YoungBae, Hiroshi Noguchi, and Masazumi Amagai. "Vibration fatigue reliability of BGA-IC package with Pb-free solder and Pb–Sn solder." *Microelectronics Reliability* 46, no. 2-4 (2006): 459-466. https://doi.org/10.1016/j.microrel.2005.02.003
[18] Bai, Ning, Xu Chen, and Hong Gao. "Simulation of uniaxial tensile properties for lead-free solders with modified Anand model." *Materials & Design* 30, no. 1 (2009): 122-128. https://doi.org/10.1016/j.matdes.2008.04.032
[19] Wilde, Jurge, Klaus Becker, Markus Thoben, Wolfgang Blum, Thomas Jupitz, Guozhong Wang, and Zhaonian N. Cheng. "Rate dependent constitutive relations based on Anand model for 92.5 Pb5Sn2. 5Ag solder." *IEEE transactions on Advanced Packaging* 23, no. 3 (2000): 408-414. https://doi.org/10.1109/6040.861554
[20] Wang, G. Z., Z. N. Cheng, K. Becker, and J. J. J. E. P. Wilde. "Applying Anand model to represent the viscoplastic deformation behavior of solder alloys." *J. Electron. Packag.* 123, no. 3 (2001): 247-253. https://doi.org/10.1115/1.1371781
[21] Bhate, Dhruv, Dennis Chan, Ganesh Subbarayan, Tz Cheng Chiu, Vikas Gupta, and Darvin R. Edwards. "Constitutive behavior of Sn3. 8Ag0. 7Cu and Sn1. 0Ag0. 5Cu alloys at creep and low strain rate regimes." *IEEE Transactions on Components and Packaging Technologies* 31, no. 3 (2008): 622-633. https://doi.org/10.1109/TCAPT.2008.2001165
[22] Basit, Munshi, Mohammad Motalab, Jeffrey C. Suhling, and Pradeep Lall. "Viscoplastic constitutive model for Lead-free solder including effects of silver content, solidification profile, and severe aging." In *International Electronic*

*Packaging Technical Conference and Exhibition*, vol. 56895, p. V002T01A002. American Society of Mechanical Engineers, 2015. https://doi.org/10.1115/IPACK2015-48619

[23] Zhang, Liang, Zhi-quan Liu, and Yu-tong Ji. "Anand constitutive model of lead-free solder joints in 3D IC device." In *Journal of Physics: Conference Series*, vol. 738, no. 1, p. 012050. IOP Publishing, 2016. https://doi.org/10.1088/1742-6596/738/1/012050